mathematics

MDPI

Article

A Surface of Section for Hydrogen in Crossed Electric and Magnetic Fields

Korana Burke [1,*,†] and Kevin Mitchell [2,†]

1 Department of Mathematics, University of California, Davis, CA 95616, USA
2 Department of Physics, University of California, Merced, CA 95344, USA; kmitchell@ucmerced.edu
* Correspondence: kburke@ucdavis.edu
† These authors contributed equally to this work.

Received: 12 August 2018; Accepted: 19 September 2018; Published: 29 September 2018

Abstract: A well defined global surface of section (SOS) is a necessary first step in many studies of various dynamical systems. Starting with a surface of section, one is able to more easily find periodic orbits as well as other geometric structures that govern the nonlinear dynamics of the system in question. In some cases, a global surface of section is relatively easily defined, but in other cases the definition is not trivial, and may not even exist. This is the case for the electron dynamics of a hydrogen atom in crossed electric and magnetic fields. In this paper, we demonstrate how one can define a surface of section and associated return map that may fail to be globally well defined, but for which the dynamics is well defined and continuous over a region that is sufficiently large to include the heteroclinic tangle and thus offers a sound geometric approach to studying the nonlinear dynamics.

Keywords: surface of section; transport; heteroclinic tangle

1. Introduction

For many dynamical systems, geometric structures lying within their phase spaces provide deep insights into their behaviors [1–3]. In particular, one class of such structures consists of homoclinic and heteroclinic tangles, which have played a crucial role in studying chaotic transport and mixing [4–11]. For dynamical systems defined by ordinary differential equations (ODEs), it is typically the case that such tangles are easiest to study when there exists a "good" surface of section (SOS) which allows one to define a continuous Poincaré return map. For two-degree-of-freedom Hamiltonian systems, a SOS is a two-dimensional surface in phase space and a heteroclinic/homoclinic tangle consists of one-dimensional stable and unstable manifolds within this surface. In many cases it is challenging, or even impossible, to define a good SOS that captures all of the dynamics of the system in question. In this paper, we will consider one such system: the dynamics of a hydrogenic electron in externally applied perpendicular (crossed) electric and magnetic fields. Though there appears to be no truly global SOS, we can define a SOS and associated Poinaré map over an area that is large enough to encompass a heteroclinic tangle that controls the ionization process.

Chaotic ionization of a hydrogenic atom in crossed electric and magnetic fields has been of scientific interest for many years [12–18]. Previous work on this problem focused on studying periodic orbits and developing closed-orbit theory in order to explain the photo-absorption spectra [19–21]. Periodic orbits were also used to construct the action variables and obtain a semiclassical torus quantization [13]. More recently, the crossed fields problem has been examined from the perspective of classical monodromy [12,16]. The electron's classical motion resembles the motion of the Moon in the Sun-Earth-Moon three body system [22], and so this system has also been considered a stepping stone to understanding escape in the classical gravitational three-body problem.

For the case in which the electric and magnetic fields are parallel, it is relatively easy to define a global SOS upon which the Poincaré map is well defined and continuous everywhere. For the crossed fields case this simple construction fails to produce a good global SOS and, to the best of our knowledge, a good global surface of section does not appear in the literature. Indeed this presents one of the major challenges to studying chaotic ionization in this case. In this paper, when we say a "good" SOS we mean an SOS that intersects all trajectories (excepting a set of measure zero) and on which the Poincaré return map is well defined and continuous everywhere, i.e., the Poincaré map is a homeomorphism of the SOS. For such good SOSs system trajectories never intersect the SOS at a tangency as this would lead to a discontinuity in the map. We will present a prescription for defining a SOS that is not truly global or continuous but is nevertheless "good enough" in that it captures all the major hallmarks of chaotic dynamics including turnstiles that govern the ionization process.

This paper is organized as follows: In Section 2 we describe equations of motion for a hydrogenic electron in crossed fields; In Section 3 we present a prescription for finding an SOS; Section 4 concludes by finding a periodic orbit and its corresponding tangle and turnstile, which are responsible for the ionization process.

2. Electron Equations of Motion

Consider an electron confined to a two-dimensional plane with a uniform magnetic field **B** oriented perpendicular to the plane. The resulting electron trajectory will be a circle. Adding an electric field **E** oriented perpendicular to the magnetic field changes the shape of the trajectory from a circle to a cycloid, i.e., the motion is a combination of the circular trajectory and an $\mathbf{E} \times \mathbf{B}$ drift. Further inclusion of a $1/r$ Coulomb potential changes the electron dynamics from regular to chaotic. This is the scenario considered in the current paper. Orienting the magnetic field in the $\hat{\mathbf{z}}$ direction and the electric field in the $\hat{\mathbf{x}}$ direction, the electron Hamiltonian in atomic units ($e = m_e = \hbar = 1$) is [14]

$$H = \frac{p^2}{2} + \frac{B}{2}L_z + \frac{B^2}{8}\left(x^2 + y^2\right) - \frac{1}{r} - Fx, \tag{1}$$

where $F = |\mathbf{E}|$ is the electric field strength, B is the magnetic field strength, and L_z is the z component of the electron's angular momentum. Equation (1) assumes a fixed infinitely massive nucleus. Since the magnetic field is oriented in the $\hat{\mathbf{z}}$ direction, it is coupled to L_z by the $BL_z/2$ term in the Hamiltonian. Since we restrict the electron motion to the xy plane, $p^2 = p_x^2 + p_y^2$, and $r = \sqrt{x^2 + y^2}$. Finally, since the Hamiltonian is independent of time, the total energy is conserved in this system.

To regularize the Coulomb singularity at the origin, we introduce the parabolic coordinates [13,21]

$$\begin{aligned} u &= \pm\sqrt{r + x}\,, & v &= \pm\sqrt{r - x}\,, \\ p_u &= vp_y + up_x\,, & p_v &= up_y - vp_x\,, \end{aligned} \tag{2}$$

where u and v are the new position variables and p_u and p_v are their corresponding conjugate momenta. We take the range of u and v to be $(-\infty, +\infty)$, which represents a double cover of the physical xy configuration space. We now define a transformed Hamiltonian h, as

$$h = 2r(H - E), \tag{3}$$

where E is the electron energy, so $h = 0$ for physically relevant trajectories. Combining Equations (1)–(3), the transformed Hamiltonian h is

$$h = \frac{1}{2}\left(p_u^2 + p_v^2\right) + \frac{B}{4}\left(u^2 + v^2\right)(up_v - vp_u) + \frac{B^2}{32}\left(u^2 + v^2\right)^3 + \frac{F}{2}\left(u^4 - v^4\right) - E\left(u^2 + v^2\right) - 2. \tag{4}$$

The transformation of the Hamiltonian in Equation (3) also transforms the time variable. The relationship between the physical time t and the transformed time s is given by

$$\frac{dt}{ds} = u^2 + v^2. \tag{5}$$

In this new coordinate system, the equations of motion are

$$\begin{aligned}
\dot{u} &= p_u - \frac{B}{4} v \left(u^2 + v^2\right) , \\
\dot{v} &= p_v + \frac{B}{4} u \left(u^2 + v^2\right) , \\
\dot{p}_u &= \frac{B}{4}\left[2uvp_u - p_v\left(3u^2 + v^2\right)\right] - \frac{3B^2}{16} u \left(u^2 + v^2\right)^2 + 2Fu^3 + 2uE , \\
\dot{p}_v &= \frac{B}{4}\left[-2uvp_v + p_u\left(u^2 + 3v^2\right)\right] - \frac{3B^2}{16} v \left(u^2 + v^2\right)^2 - 2Fv^3 + 2vE ,
\end{aligned} \tag{6}$$

where the overdot represents differentiation with respect to s.

Finally, we introduce the vectors $\mathbf{p}$, $\mathbf{w}$, and $\mathbf{A}$

$$\mathbf{p} = [p_u, p_v] , \tag{7}$$

$$\mathbf{A} = \frac{1}{4} B \left(u^2 + v^2\right) [v, -u] , \tag{8}$$

$$\mathbf{w} = [\dot{u}, \dot{v}] = \mathbf{p} - \mathbf{A} , \tag{9}$$

which allows us to rewrite the Hamiltonian in parabolic coordinates in a more compact form

$$h = \frac{1}{2} |\mathbf{p} - \mathbf{A}|^2 - E\left(u^2 + v^2\right) - \frac{1}{2} F \left(u^4 - v^4\right) - 2 \tag{10}$$

$$= \frac{1}{2} |\mathbf{w}|^2 - E\left(u^2 + v^2\right) - \frac{1}{2} F \left(u^4 - v^4\right) - 2 . \tag{11}$$

The explicit dependence on the electric field strength F can be removed by rescaling the lengths by $F^{1/2}$, momenta by $F^{-1/4}$, time by $F^{3/4}$, magnetic field by $F^{-3/4}$, and the energy by $F^{-1/2}$. The resulting effect on Equation (10) is equivalent to setting $F = 1$. The system then depends on only two independent parameters: the magnetic field strength B and the electron energy E.

3. Construction of the Surface of Section

A global surface of section is easy to find for the case of hydrogen in *parallel* electric and magnetic fields. In that case the Hamiltonian can again be transformed using parabolic coordinates as in Section 2 yielding an effective Hamiltonian

$$h = \frac{1}{2}\left(p_u^2 + p_v^2\right) - E\left(u^2 + v^2\right) + \frac{1}{8} B^2 \left(u^4 v^2 + u^2 v^4\right) - \frac{1}{2}\left(u^4 - v^4\right) - 2 . \tag{12}$$

In this case, the Hamiltonian can be decomposed into kinetic plus potential terms with no vector potential in the kinetic term. The shape of the potential guarantees that any trajectory launched from the u-axis will return to the u-axis crossing it transversely. Furthermore, every trajectory will intersect the u-axis an infinite number of times. We therefore can use the u-axis to construct the SOS; the SOS within the full four-dimensional phase space is the two-dimensional surface within the energy shell $h = 0$ that projects to the u-axis. This surface has two connected components: one for trajectories moving upward through the u-axis, and one for trajectories moving downward through the u-axis. We formally identify these two components via reflection symmetry about the u-axis. The SOS thus has canonical coordinates (u, p_u). The corresponding Poincaré map returns the value of the coordinates (u, p_u) each time a trajectory crosses the u-axis, going either upward or downward [23–25].

We can try the same approach in the crossed fields problem, defining a SOS with the u-axis. However, this approach fails due to the presence of the vector potential term in Equation (10). A trajectory launched tangent to the u-axis will curve away from it both forward and backward in time, due to the presence of the magnetic field; this launch point thus constitutes a tangential intersection with the u-axis (See Figure 1). Furthermore, the $\mathbf{E} \times \mathbf{B}$ drift causes some trajectories to never return to the u-axis (Figure 1). Hence this SOS definition would suffer both from tangencies and the failure to capture all possible trajectories.

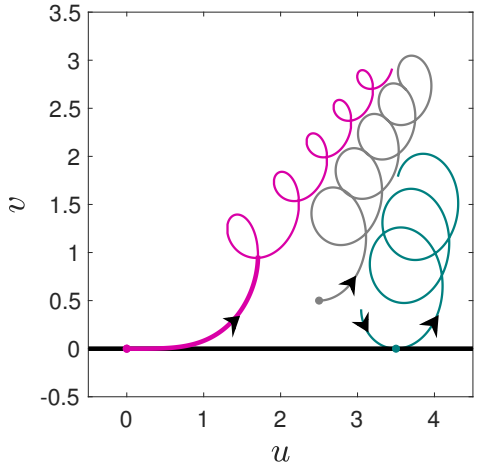

Figure 1. Three representative trajectories. Teal curve is the trajectory launched tangent to the u-axis away from the nucleus. Grey curve represents a trajectory launched off the u-axis away from the nucleus. Magenta trajectory is the trajectory launched away from the nucleus along the u-axis. The thick magenta curve represents the portion of the trajectory used to define the surface of section (SOS). ($B = 2$, $E = -1.1$, where B and E are the magnetic field strength and the energy in scaled coordinates.)

Returning to the parallel fields problem, we need to think more deeply about why the u-axis generates a good SOS in the parallel fields problem. For parallel fields, a trajectory launched tangent to the u-axis does not create a tangential intersection with the u-axis because it remains on the u-axis, that is, the u-axis is itself a trajectory of the system. This is true regardless of the magnitude of the momentum and whether the momentum points to the left or right. We adapt this idea for the crossed fields problem by choosing the trajectory that begins at the nucleus (located at $u = v = 0$) and is launched away from the nucleus along the u-axis to the right as shown in Figure 1. Locally at the nucleus this trajectory corresponds to the trajectory used to define the Poincaré return map in the parallel fields case. As the electron moves away from the nucleus, the electric and magnetic fields create a trajectory that resembles a tapered cycloid with the larger radius closer to the nucleus.

Notice that when projected onto the uv-space this trajectory self intersects. Nevertheless, we take the portion of the trajectory shown as bold in Figure 1 from the nucleus ($u = v = 0$) up to the point where the tangent to the trajectory points in the v direction in uv-space. (One could extend the trajectory up to the second time the trajectory passes through the first self-intersection point. However for ease of implementation, we are using a simpler criterion of cutting off the trajectory at the first vertical tangent line.) Next, we replicate this portion of the trajectory into the remaining quadrants in uv-space, by first reflecting through the origin and then reflecting about the horizontal axis (See Figure 2). Reflecting through the origin corresponds to launching a trajectory from the nucleus along the u-axis to the left. On the other hand, reflecting about the u-axis is equivalent to time reversal giving two trajectories that move toward the nucleus. In Figure 2, we show portions of the trajectories launched away from the nucleus in blue, and the time-reversed partners in red. We call these the SOS curves. The arrows denote the direction of time along the trajectory. Thus, a trajectory comes in towards the nucleus from the upper left and continues smoothly into the trajectory in the upper right.

Similarly a trajectory comes in from the lower right and exits on the lower left. These two trajectories are analogous to trajectories moving either left or right along the u-axis in the parallel fields case. In the parallel fields case these trajectories lie on top of one another, whereas here the vector potential splits them into separate curves.

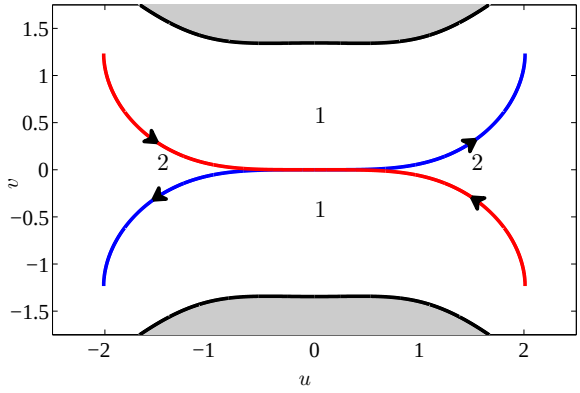

Figure 2. Trajectories defining the SOS ($B = 1.5$, $E = -0.2$). The thick black line represents the boundary between the energetically allowed (white) and forbidden (shaded) regions. Crossing either red or blue curves from region labeled 1 to region labeled 2 defines the SOS. Trajectories that cross from region 2 to region 1 are not part of the SOS.

The SOS is now defined by recording the electron's position and momentum whenever an electron trajectory intersects either the red or the blue curves while moving from the region labeled 1 to the region labeled 2. We do not consider crossings from region 2 to region 1 as part of the SOS. Thus we only consider upward propagating trajectories on the lower right and downward propagating trajectories on the upper right. For the parallel fields problem these two branches were identified, but this is no longer possible in the crossed fields case due to the broken time-reversal symmetry. Nevertheless, the picture can be simplified by taking advantage of another symmetry. There remains a reflection symmetry through the origin in which the upper left branch is identified with the lower right branch, and the lower left branch is identified with the upper right branch. We therefore compose the SOS from just the two branches on the right.

This definition of the SOS is free of tangencies for any trajectory approaching from region 1. This is because the curve that defines the SOS is a portion of a physical trajectory. To show this, suppose a trajectory does intersect the SOS transversely at an isolated point $\mathbf{d_0} = [u, v]$. Then the direction of the velocity $\mathbf{w} = [\dot{u}, \dot{v}]$ is determined up to a minus sign at r. Furthermore, since the trajectory has a fixed energy E, the magnitude of the velocity at $\mathbf{d_0}$ is determined by setting Equation (11) equal to zero and solving for $|\mathbf{w}|$. Thus, the velocity vector $\mathbf{w}$ is determined up to a minus sign. If the direction of $\mathbf{w}$ coincides with the direction of the trajectory used to define the SOS, then by the uniqueness of the ODE solution, the two trajectories are the same and the intersection $\mathbf{d_0}$ is not an isolated point. Hence, we take $\mathbf{w}$ to point in the opposite direction. In this case, the trajectory will curve in the opposite direction as the SOS curve, as shown in Figure 3. Therefore it intersects the SOS curve coming from region 2. Thus, no trajectory coming from region 1 can intersect the SOS tangentially.

We next introduce canonical coordinates in two-dimensional SOS. We define the position variable a to be the Euclidean length along the SOS trajectory as measured from the nucleus. Positive a parametrizes the curve in the upper right quadrant, and negative a parametrizes the curve in the lower right quadrant. The momentum coordinate p_a is defined by projecting the momentum (p_u, p_v) onto the tangent line to the SOS trajectory.

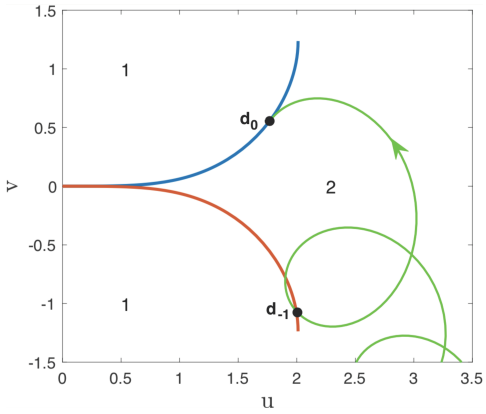

Figure 3. Green curve represents the trajectory which maps the point $\mathbf{d_{-1}}$ on the portion of the red SOS curve to the tangency $\mathbf{d_0}$ on the blue portion of the SOS curve.

We now define the Poincaré return map $(a, p_a) \mapsto (a', p_a')$ in the following way. Given (a, p_a) we begin a trajectory at position a along the SOS trajectory and with the tangential momentum given by p_a. We determine $|\mathbf{w}|$ by setting Equation (11) equal to zero. Please note that the tangential component of velocity is given by $\mathbf{w} \cdot \hat{\mathbf{t}} = p_a - \mathbf{A} \cdot \hat{\mathbf{t}}$, where $\hat{\mathbf{t}}$ is the unit tangent pointing forward along the SOS trajectory (Equation (9)). Thus, the perpendicular component of velocity is given by $w_\perp = \pm\sqrt{|\mathbf{w}|^2 - \left(p_a - \mathbf{A} \cdot \hat{\mathbf{t}}\right)^2}$. The sign of $w_\perp$ is determined by requiring the normal component of $\mathbf{w}$ to point from region 1 to region 2 in Figure 2. This uniquely determines $\mathbf{w}$, which uniquely determines $\mathbf{p}$ via Equation (9). Now that an initial point (u, v, p_u, p_v) in the full phase space has been determined, we evolve Hamilton's Equations (6) forward until the trajectory intersects one of the four branches in Figure 2 traveling from region 1 into region 2. If the intersection is with one of the two left branches, we reflect the point and its momentum through the origin, i.e., $(u, v, p_u, p_v) \mapsto -(u, v, p_u, p_v)$. At this point we record the coordinates (a', p_a') on the SOS. Please note that some trajectories will never return to the SOS since the SOS is not globally defined. Such trajectories are easy to identify because they spiral outward toward infinity, escaping the nucleus. See Figure 1.

A set of sample SOS plots is shown in Figure 4. One can notice the presence of periodic orbits and stable islands immersed in the chaotic sea.

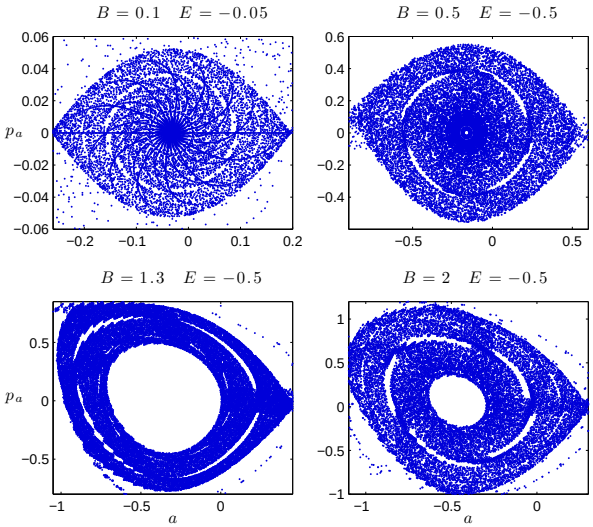

Figure 4. A sample of SOS plots for different values of the magnetic field strength and energy. The values of the magnetic field B and the energy of the ensemble E are marked on top of the figures. Electric field strength F is set to 1 in all four figures.

4. Visualizing a Periodic Orbit and Its Tangle

The ionization dynamics of this system is governed by a symmetric pair of periodic orbits in the left and right saddle regions of the potential in uv-space. (See Figure 5) In the original xy-coordinates these two periodic orbits are identified into a single orbit near the Stark saddle. In uv-space this orbit intersects the SOS curves in four places, but only two of those places intersect the SOS because the orbit must move from region 1 to region 2 as marked with black dots in Figure 6. These two intersection points form a period-2 orbit of the Poincaré map. This period-2 orbit is hyperbolic. Figure 7 shows a summary of the main results of this paper. The hyperbolic period-2 point has stable and unstable manifolds, shown in red and blue respectively, which intersect to form a heteroclinic tangle. Importantly the SOS for the parameters shown in Figure 7 is large enough to include not only the period-2 orbit but also the entire resonance zone defined by the tangle. The resonance zone is the domain bounded by the segments of the stable manifold (red) connecting z_R to p_0 and z_L to p_1 and by the segments of the unstable manifold (blue) connecting z_R to p_1 and z_L to p_0.

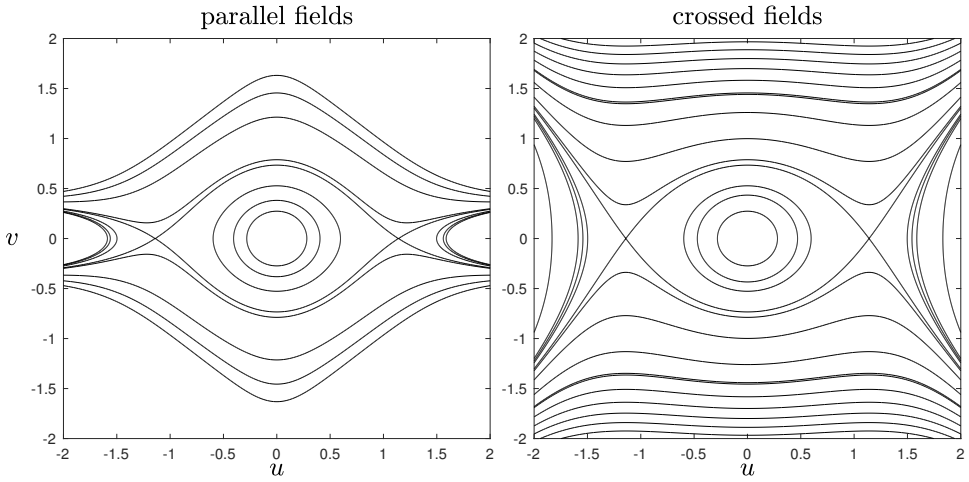

Figure 5. Left figure shows the potential for the parallel fields case, and the right figure shows the potential for the crossed fields case. ($E = -1.3$, and $B = 4.5$.)

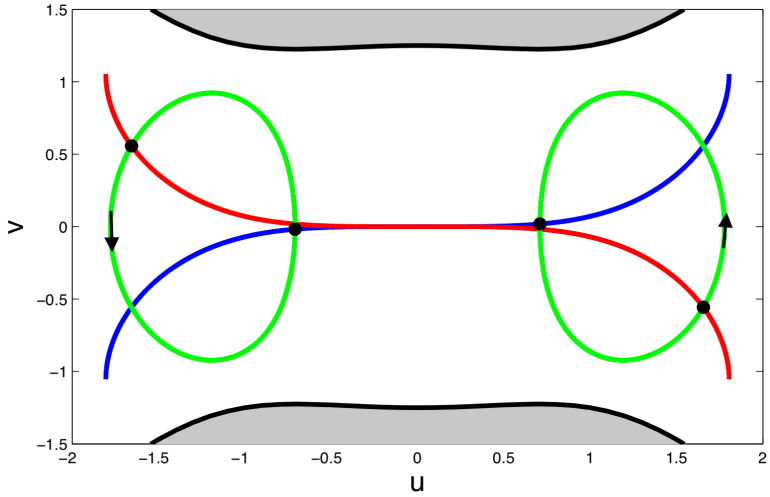

Figure 6. Symmetric unstable periodic orbits are shown in green. Two pairs of black dots mark the intersections of the periodic orbit with the SOS. The thick black line represents the boundary between the energetically allowed (white) and forbidden (shaded) regions.

The heteroclinic tangle defines regions in phase space called lobes, which fall into two categories: those governing the escape from the resonance zone, labeled E_k, and those governing the capture into the resonance zone, labeled C_k. (See Figure 7.) The escape lobe E_0, which is inside the resonance zone, maps to the E_1 lobe, which is outside the resonance zone. Similarly, the capture lobe C_{-1}, which is outside the resonance zone, maps to the C_0 lobe, which is inside. These lobes define a phase space turnstile which governs the ionization process [6].

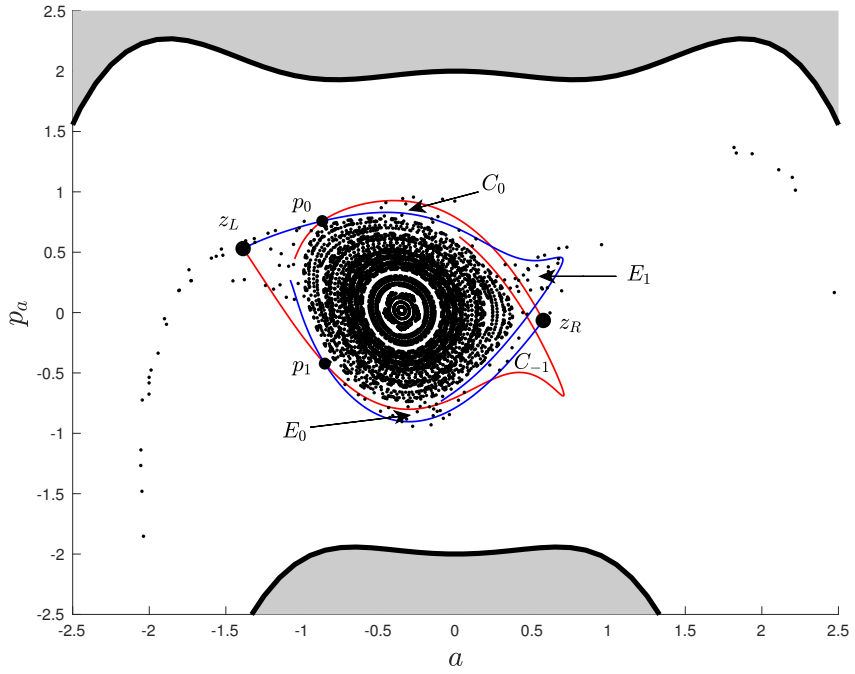

Figure 7. Surface of Section for $B = 1.5$, $E = -0.5$. Two big black dots represent the unstable period two orbit. The red line is the portion of the stable manifold, and the blue line is the portion of the unstable manifold. Thick black line defines the boundary between the energetically allowed (white) and forbidden (shaded) regions.

We now return to discuss the issue of tangencies and discontinuities in the Poincaré map. As mentioned before, there are no trajectories that intersect the SOS tangentially coming from region 1. However, in general there may be trajectories that map from the SOS to a tangential intersection with the SOS coming from region 2. See Figure 3. At any point on the SOS, i.e., at any value of the a coordinate, these tangential intersections correspond to the minimum value of momentum p_a. That is, the tangential intersections form the lower black boundary of the physically allowed domain in Figure 7. Thus, the Poincaré map will be continuous on any topological disk D that maps forward to a domain that does not intersect the lower boundary of the physically allowed region. It is enough to check just the boundary of the domain D. That is, if the boundary of a domain D maps forward to a closed curve that does not intersect the lower boundary of the physically allowed region, then the Poincaré map is continuous over the entire domain D. The resonance zone of the tangle in Figure 7 satisfies this property, and thus the Poincaré map is continuous over the entire resonance zone. The same argument applies to the inverse Poincaré map.

To complete the picture, we have also included additional orbits (represented by black dots) that are contained inside the heteroclinic tangle. One can observe a similar prominent chain of stable islands contained inside this heteroclinic tangle as the one shown in Figure 4. It is important to note that it is the heteroclinic tangle attached to the periodic orbit furthest away from the nucleus that governs the ionization process. Any additional heteroclinic tangles that might exist in the system would be contained inside this outermost tangle.

As we have mentioned earlier, this SOS is not defined globally. For any given set of parameter values, there are always trajectories that do not return to the SOS. For some set of parameter values, the SOS is large enough to encompass the whole of the resonance zone of the heteroclinic tangle. However, this does not hold for all parameter values but only for a certain range of magnetic field strength and energy. Two opposing effects determine the range of validity: the Euclidean distance from the nucleus where the trajectory has its first vertical tangent when projected to the uv-space, and the position of the unstable periodic orbit. For a fixed value of electron energy increasing the magnetic field decreases the Larmor radius of the SOS trajectory we use to define the Poincaré SOS and hence decreases the range of the a coordinate in the local SOS. At the same time the unstable period-two orbit moves away from the nucleus, and hence it its a coordinate increases, until it finally "slips off" the SOS. Figure 8 shows the B-dependance of the position of the periodic orbit and the edge of the SOS definition. For a critical value of the magnetic field strength, the periodic orbit falls off the surface of section, and this ceases to be a useful local SOS for representing the heteroclinic tangle structure. This happens at the value of B for which the blue and the green curves meet in Figure 8. (For $E = -0.5$ this failure occurs at $B = 1.91$.)

Since the portion of phase space that has been promoted from bound to ionized via a turnstile never returns to the bound state, we argue that the local SOS is sufficient if one is interested in studying the chaotic ionization mechanism in this system.

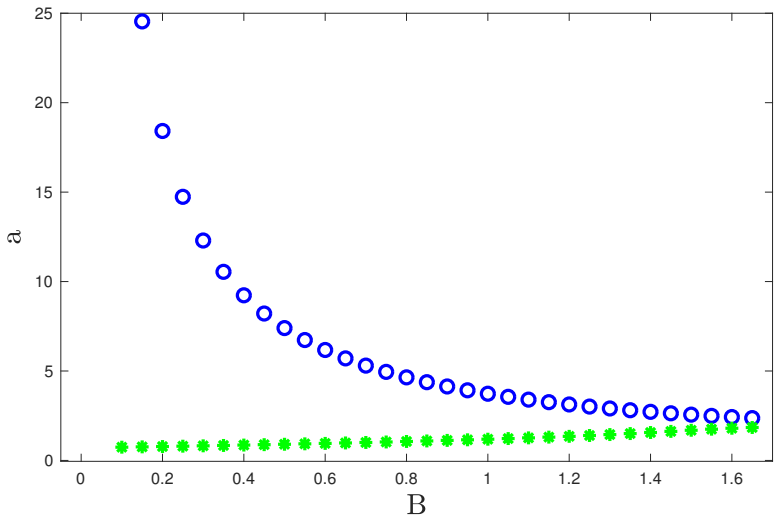

Figure 8. The blue dots represent the value of a at the edge of the surface of section, and the green stars represent the largest of the two absolute a values for the periodic orbit. ($E = -0.5$)

5. Conclusions

We have provided a prescription for defining a local surface of section for a nonlinear system whose global surface of section is not known and may not exist. This local surface of section allows us to capture all the main hallmarks of a chaotic system: an unstable periodic orbit, the most important pieces of the heteroclinic tangle attached to the unstable periodic orbit, the phase space turnstile that leads to ionization, as well as stable islands embedded in the chaotic sea. These structures can then be used for future applications such as the construction of the symbolic dynamics using the homotopic lobe dynamics approach, computation of topological entropy, periodic orbit computations of escape rates and spectral oscillations in the density of states [3,19,20]. One of the reasons why this technique works, which may be relevant for other applications, is that defining the SOS using an orbit of the system eliminates tangencies from trajectories propagating in the same direction as the SOS trajectory. Even though this approach fails for large magnetic field values, we believe it still offers valuable insights into studying types of problems where one is unable to define a global surface of section.

It would be interesting to see if this approach works in the circular restricted gravitational three-body problem as well.

Author Contributions: Conceptualization, K.B. and K.M.; Methodology, K.B. and K.M.; Software, K.B. and K.M., Validation, K.B. and K.M.; Formal Analysis, K.B. and K.M.; Writing-Original Draft Preparation, K.B. and K.M.; Writing-Review and Editing, K.B. and K.M.; Visualization, K.B. and K.M.; Funding Acquisition, K.M.

Funding: This work was supported in part by NSF grants PHY-0748828 and PHY-1408127. This material is based in part upon work supported by the National Science Foundation under Grant No. DMS-1440140 while the second author was in residence at the Mathematical Sciences Research Institute in Berkeley, California, during the Fall 2018 semester.

Conflicts of Interest: The authors declare no conflict of interest.

References

1. Strogatz, S. *Nonlinear Dynamics and Chaos: With Applications to Physics, Biology, Chemistry, and Engineering*; CRC Press: Boca Raton, FL, USA, 2018.
2. Meiss, J. *Differential Dynamical Systems, Revised Edition*; Mathematical Modeling and Computation, Society for Industrial and Applied Mathematics: Philadelphia, PA, USA, 2017.
3. Cvitanović, P.; Artuso, R.; Mainieri, R.; Tanner, G.; Vattay, G. *Chaos: Classical and Quantum*; Niels Bohr Inst.: Copenhagen, Denmark, 2016.
4. Wiggins, S. *Chaotic Transport in Dynamical Systems*; Springer: New York, NY, USA, 1992.
5. Rom-Kedar, V. Transport rates of a class of two-dimensional maps and flows. *Physica D* **1990**, *43*, 229–268. [CrossRef]
6. Mackay, R.; Meiss, J.; Percival, I. Transport in Hamiltonian systems. *Physica D* **1984**, *13*, 55–81. [CrossRef]
7. Jung, C.; Emmanouilidou, A. Construction of a natural partition of incomplete horseshoes. *Chaos* **2005**, *15*, 023101. [CrossRef] [PubMed]
8. Collins, P. Dynamics forced by surface trellises. In *Contemporary Mathematics: Geometry and Topology in Dynamics*; American Mathematical Society: Providence, RI, USA, 1999; pp. 65–86.
9. Collins, P. Symbolic Dynamics from homoclinic tangles. *Int. J. Bifurc. Chaos* **2002**, *12*, 605–617. [CrossRef]
10. Collins, P. Forcing Relations for Homoclinic Orbits of the Smale Horseshoe Map. *Exp. Math.* **2005**, *14*, 75–86. [CrossRef]
11. Burke, K.; Mitchell, K.A. Chaotic ionization of a Rydberg atom subjected to alternating kicks—The role of phase space turnstiles. *Phys. Rev. A* **2009**, *80*, 033416. [CrossRef]
12. Cushman, R.; Sadovskiĭ, D. Monodromy in the hydrogen atom in crossed fields. *Physica D* **2000**, *142*, 166–196. [CrossRef]
13. Gekle, S.; Main, J.; Bartsch, T.; Uzer, T. Hydrogen atom in crossed electric and magnetic fields: Phase space topology and torus quantization via periodic orbits. *Phys. Rev. A* **2007**, *75*, 023406. [CrossRef]
14. Jaffé, C.; Farrelly, D.; Uzer, T. Transition State Theory without Time-Reversal Symmetry: Chaotic Ionization of the Hydrogen Atom. *Phys. Rev. Lett.* **2000**, *84*, 610–613. [CrossRef] [PubMed]
15. Von Milczewski, J.; Uzer, T. Chaos and order in crossed fields. *Phys. Rev. E* **1997**, *55*, 6540–6551. [CrossRef]
16. Schleif, C.R.; Delos, J.B. Monodromy and the structure of the energy spectrum of hydrogen in near perpendicular electric and magnetic fields. *Phys. Rev. A* **2007**, *76*, 013404. [CrossRef]
17. Wiebusch, G.; Main, J.; Krüger, K.; Rottke, H.; Holle, A.; Welge, K.H. Hydrogen atom in crossed magnetic and electric fields. *Phys. Rev. Lett.* **1989**, *62*, 2821–2824. [CrossRef] [PubMed]
18. Raithel, G.; Fauth, M.; Walther, H. Atoms in strong crossed electric and magnetic fields: Evidence for states with large electric-dipole moments, *Phys. Rev. A* **1993**, *47*, 419–440. [CrossRef]
19. Du, M.L.; Delos, J.B. Effect of closed classical orbits on quantum spectra: Ionization of atoms in a magnetic field. I. Physical picture and calculations. *Phys. Rev. A* **1988**, *38*, 1896–1912. [CrossRef]
20. Gao, J.; Delos, J.B.; Baruch, M. Closed-orbit theory of oscillations in atomic photoabsorption cross sections in a strong electric field. I. Comparison between theory and experiments on hydrogen and sodium above threshold. *Phys. Rev. A* **1992**, *46*, 1449–1454. [CrossRef] [PubMed]
21. Wang, D.M.; Delos, J.B. Organization and bifurcation of planar closed orbits of an atomic electron in crossed fields. *Phys. Rev. A* **2001**, *63*, 043409. [CrossRef]

22. Flöthmann, E.; Welge, K.H. Crossed-field hydrogen atom and the three-body Sun-Earth-Moon problem. *Phys. Rev. A* **1996**, *54*, 1884–1888. [CrossRef] [PubMed]
23. Mitchell, K.A.; Handley, J.P.; Tighe, B.; Flower, A.; Delos, J.B. Analysis of chaos-induced pulse trains in the ionization of hydrogen. *Phys. Rev. A* **2004**, *70*, 043407. [CrossRef]
24. Mitchell, K.A.; Handley, J.P.; Tighe, B.; Flower, A.; Delos, J.B. Chaos-Induced Pulse Trains in the Ionization of Hydrogen. *Phys. Rev. Lett.* **2004**, *92*, 073001. [CrossRef] [PubMed]
25. Mitchell, K.A.; Delos, J.B. The structure of ionizing electron trajectories for hydrogen in parallel fields. *Physica D* **2007**, *229*, 9–21. [CrossRef]